

# Signal, orbit and attitude analysis of Japan's first QZSS satellite Michibiki

André Hauschild · Peter Steigenberger ·  
Carlos Rodriguez-Solano

Received: 4 November 2011 / Accepted: 10 November 2011 / Published online: 9 December 2011  
© Springer-Verlag 2011

**Abstract** Results are presented for Michibiki, the first satellite of Japan's Quasi-Zenith Satellite System. Measurements for the analysis have been collected with five GNSS tracking stations in the service area of QZSS, which track five of the six signals transmitted by the satellite. The analysis discusses the carrier-to-noise density ratio as measured by the receiver for the different signals. Pseudorange noise and multipath are evaluated with dual-frequency and triple-frequency combinations. QZSS uses two separate antennas for signal transmission, which allows the determination of the yaw orientation of the spacecraft. Yaw angle estimation results for an attitude mode switch from yaw-steering to orbit-normal orientation are presented. Estimates of differential code biases between QZSS and GPS observations are shown in the analysis of the orbit determination results for Michibiki. The estimated orbits are compared with the broadcast ephemerides, and their accuracy is assessed with overlap comparisons.

**Keywords** QZSS · Michibiki · QZS-1 · CONGO · Multipath analysis · Yaw attitude estimation · Orbit determination

---

The GNSS In Progress column is dedicated to current issues and latest advances in the area of GNSS and accepts short contributions. The Column Editor is Dr. Oliver Montenbruck (oliver.montenbruck@dlr.de) of the German Space Operations Center (DLR/GSOC), who can be contacted prior to submission if necessary.

---

A. Hauschild (✉)  
German Space Operations Center,  
Deutsches Zentrum für Luft-und Raumfahrt (DLR),  
Wessling, Germany  
e-mail: andre.hauschild@dlr.de

P. Steigenberger · C. Rodriguez-Solano  
Institut für Astronomische und Physikalische Geodäsie,  
Technische Universität München, Munich, Germany

## Quasi-Zenith Satellite System overview and tracking network

Japan's Quasi-Zenith Satellite System (QZSS) is a regional augmentation system, which provides GPS compatible signals as well as integrity information and differential corrections. The first satellite Michibiki, or QZS-1, has been launched on September 11, 2010 and is depicted in Fig. 1. The complete constellation will consist of three satellites with a common ground path. The geosynchronous, inclined, elliptical orbits are designed to provide extended visibility periods of the satellite with high elevation angles over Japan. The first main objective of the new constellation is the availability enhancement of positioning solutions in challenging environments like urban canyons. For this purpose, the QZSS satellites offer four signals (C/A, L1C, L2C and L5), which are interoperable with GPS and allow for the combined processing of both systems. The second objective is the enhancement of the real-time navigation accuracy and reliability. Two dedicated signals of QZSS provide integrity and correction information. The Submeter-class Augmentation with Integrity Function (SAIF) signal is broadcast on L1 from a dedicated transmit antenna onboard the satellite. It contains wide area differential correction data (Kishimoto et al. 2011). The L-band experimental (LEX) signal is broadcast at the center frequency of the GALILEO E6 frequency (1278.75 MHz) and contains high-precision corrections for GPS satellite clock and orbit errors, tropospheric and ionospheric delays (Kishimoto et al. 2011, Saito et al. 2011).

A subset of receivers of the COoperative Network for GIOVE Observations (CONGO) (Montenbruck et al. 2011a) has been upgraded shortly after the first signals have been emitted by QZS-1. The stations are located in Chofu, Japan (CHOF), Singapore (SING), Sydney, Australia (UNSX),



**Fig. 1** Michibiki (or QZS-1), the first QZSS satellite (imagery courtesy: JAXA)

Maui, Hawaii (MAHO) and Papeete, Tahiti (THTX). All sites are equipped with Javad TRE-G3TH receivers and are connected to geodetic antennas. The receivers are able to track GPS, GLONASS, GIOVE, SBAS and QZSS signals. For the latter, all signals except for LEX are supported. The analysis provided is based on the measurements from the five CONGO stations (Fig. 2).

**Carrier-to-noise density ratio**

Figure 3 depicts the carrier-to-noise density ratio ( $C/N_0$ ) for QZS-1 and GPS as a function of satellite elevation as measured by the TRE-G3TH receiver in Chofu, Japan. Measurements for a period of 3 days from July 8 to 10, 2011, have been used. Only the first Block IIF satellite SVN 62 and all Block IIR-M satellites except for SVN 49 have been included in this analysis. It becomes obvious that the C/A code signals of GPS are approximately 4–5 dB more powerful than the signal of QZS-1 over the entire elevation range. A similar result is found for L5, where the curve for GPS is about 2 dB higher compared with QZSS. It should be noted at this point that SVN 62 is the only satellite contributing to L5 for GPS. The carrier-to-noise density ratio for L2C, on the other hand, has a comparable

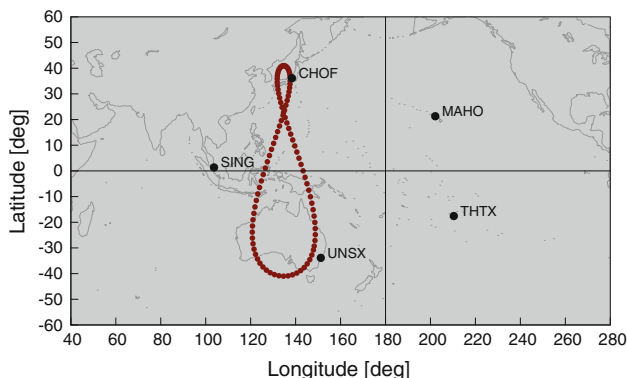


**Fig. 2** Tracking stations of the CONGO network with QZSS tracking capabilities. The ground track of QZSS is indicated as a dotted line with a step size of 15 min

level for both systems at low to medium elevation angles. However, close to zenith the received signal for QZSS is approximately 1.5–2 dB less powerful compared with GPS.

Since the QZSS signals are GPS compatible signals, the attenuations and amplifications in the antenna and the receiver are identical to GPS. Therefore, the differences in the  $C/N_0$  levels for QZSS and GPS result from actual differences in the power level or transmit antenna gain pattern at the satellite. It is furthermore interesting to note that due to the high eccentricity of the QZSS orbit, the orbit height differs by approximately 6,300 km between apogee over the northern hemisphere and perigee over the southern hemisphere. Correspondingly, the path loss for the satellite at zenith changes from  $-161.27 \text{ dB/m}^2$  at perigee to  $-162.81 \text{ dB/m}^2$  at apogee. As a result, receivers tracking QZS-1 at zenith in the southern hemisphere receive higher signal power than receivers in the northern hemisphere under the same tracking conditions. However, this orbit design is advantageous for users in Japan, since the satellite remains longer in the northern hemisphere than in the southern hemisphere.

**Noise and multipath analysis**

For the analysis of pseudorange noise and multipath errors, the multipath (MP) combination (Kee and Parkinson 1994) is computed from

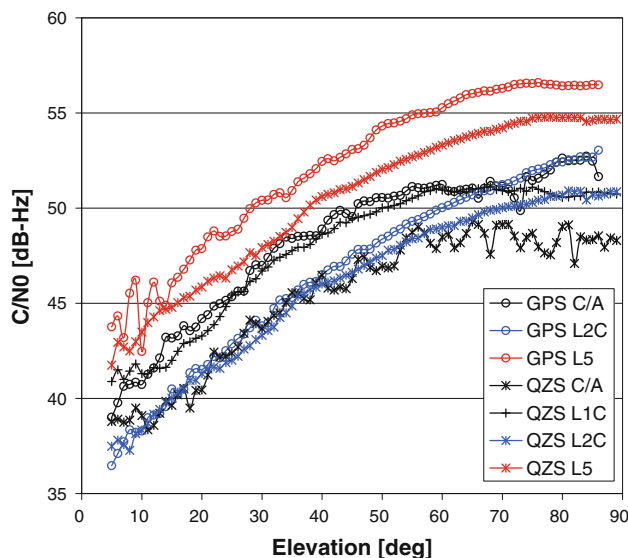


**Fig. 3** Carrier-to-noise density ratios as a function of satellite elevation for a Trimble Zephyr Geodetic 2 antenna (station CHOF) for GPS and QZSS L1 (black), L2 (blue) and L5 (red) signals for a 3-day period from July 8–10, 2011. Satellites contributing to GPS data are limited to the first Block IIF satellite SVN 62 and the Block IIR-M satellites except for SVN 49

$$MP_A = \rho_A - (a + 1) \cdot \Phi_A + a \cdot \Phi_B + b$$

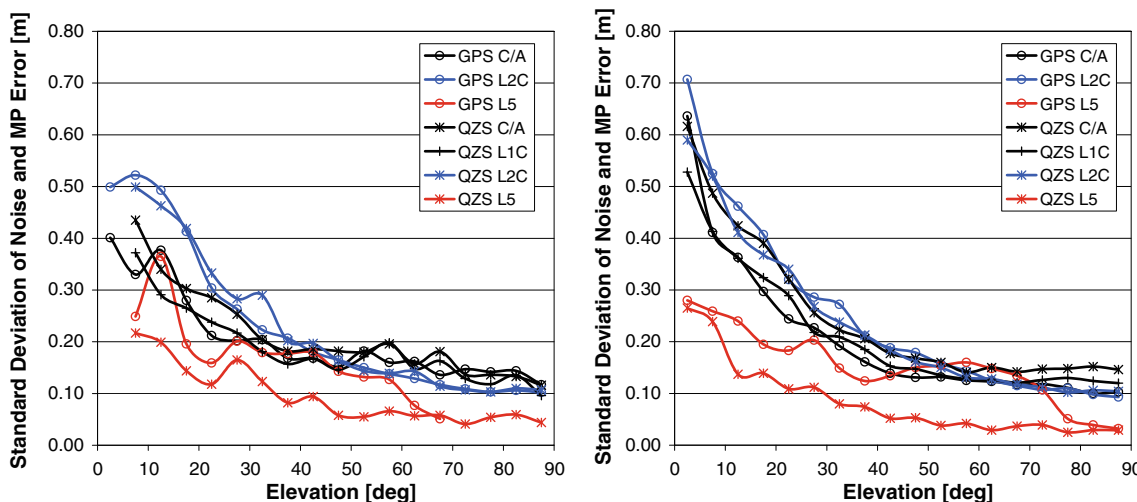
with  $a = 2 \cdot f_B^2 / (f_A^2 - f_B^2)$

where  $MP_A$  is the code multipath of the signal A,  $\rho_A$  and  $\Phi_A$  are pseudorange and carrier phase on signal A,  $\Phi_B$  is a carrier phase on signal B and  $b$  is a bias. The corresponding frequencies are  $f_A$  and  $f_B$ . This combination eliminates all errors except for receiver noise, multipath errors and bias variations from the pseudorange observation. Results of the MP combination of C/A, L1C, L2C and L5 for the station in Sydney (UNSX) and Chofu (CHOF) are depicted in Fig. 4. The station UNSX is equipped with a TRE-G3TH receiver and a Leica AR25.R3 antenna. CHOF uses the same receiver but a Trimble Zephyr Geodetic 2 antenna. The plots show the standard deviation of the multipath combination over satellite elevation. The MP combination of signals on L1 has been formed with the carrier phase from L2, the L2C and L5 MP combinations have been formed with the carrier phase from L1. QZS-1 and all GPS satellites except for SVN 49 (PRN 01) have been used in this analysis.

It becomes obvious that the L5 signals for QZS exhibit the lowest noise and multipath errors for both stations. This superior performance could be suspected since the L5 signal has the highest chip rate with 10.23 Mbps and is therefore least susceptible to multipath. The standard deviation is on the order of 5 cm or less for high elevation angles. In comparison, the GPS L5 multipath and receiver noise are significantly larger for both receivers. This is an unexpected result, since both signals are interoperable and should yield the same multipath performance. However, it must be kept in mind that the statistics for the GPS L5 multipath combination are based on the observations from

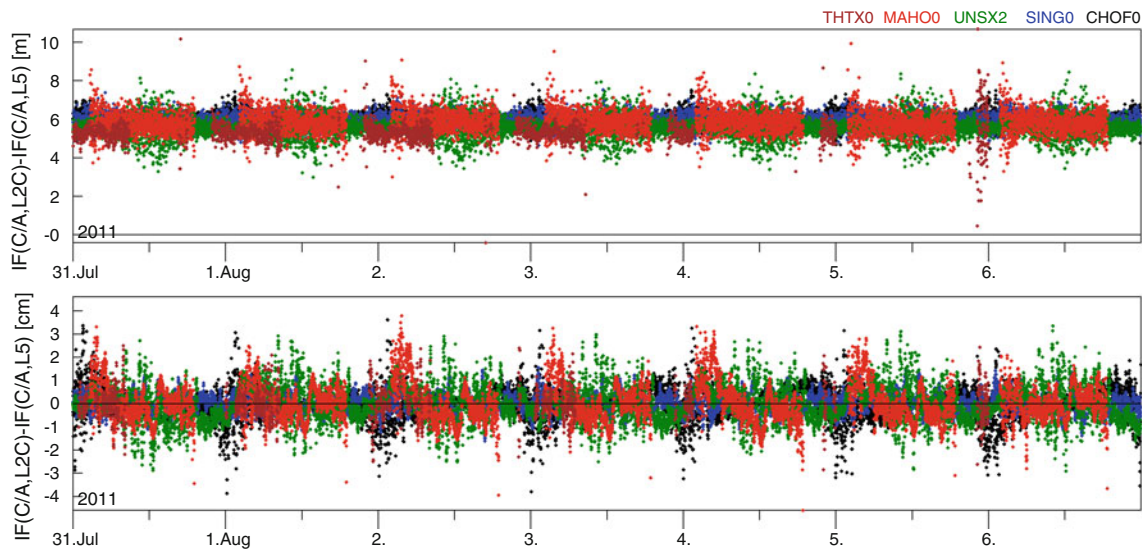
a single Block IIF satellite only, which is obviously affected by higher multipath compared with Michibiki. For the L2C signal, the multipath performance for GPS and QZSS is comparable for both stations. The standard deviation reaches a level of 10 cm for high elevations in both cases. However, at elevation angles of less than 10°, the station in Chofu seems to be affected by higher multipath and noise. The C/A code signals for GPS and QZSS also exhibit comparable performance. At Chofu, the multipath and receiver noise for QZSS C/A is approximately 60 cm at 5° elevation and about 15 cm at zenith. GPS C/A code has a similar performance at 5° elevation but exceeds QZSS for higher elevation angles and reaches a level of 10 cm at zenith. At UNSX, the errors are smaller compared with CHOF at low elevation angles. For higher elevation angles, both GPS and QZSS reach a level of 15 cm. It is interesting to note that L1C, which is only available for QZSS, has a superior performance at both stations compared with the C/A code signals.

Figure 5 depicts a triple-frequency combination of the C/A, L2C and L5 pseudorange and carrier phase measurements of QZS-1 over a period of 1 week. The combination used for this plot is equivalent to the difference of the ionosphere-free (IF) combination of C/A code and L2C and the IF combination of C/A code and L5. It eliminates all effects due to geometry, clock offsets, troposphere and ionosphere (Montenbruck et al. 2011b). The top plot in Fig. 5 shows the combination of the pseudorange observables of all five CONGO stations supporting QZSS. The triple-frequency code combinations for all stations are offset by roughly 6 m with small difference between the individual stations. This offset is due to code biases of the individual signals, which do not cancel out. Even though



**Fig. 4** Standard deviation of the noise and multipath error of the multipath combination for GPS and QZSS signals for station UNSX (left plot) and CHOF (right plot). Observations from a period of 5

days from July 13–17, 2011, have been used. For GPS, all satellites except for SVN49 (PRN01) are used. Note that only SVN62 (PRN25) contributes to the GPS L5 signal



**Fig. 5** Triple-frequency combination of QZSS pseudoranges (*top*) and carrier phases (*bottom*) for a period of 1 week from July 31 to August 6, 2011

all stations use identical receivers and firmware, the differences in the linear combination of code biases can be explained from different cabling and amplifiers. The bottom plot depicts the combination of carrier phase observations, where the linear combination of ambiguities has been removed for each pass. The higher resolution of the carrier phase makes systematic variations visible, which exhibit a daily repeatability and are uncorrelated between the stations. These effects are most prominent for the station MAHO at noon of each day. A possible explanation for the variations is a change in receiver line biases over time. However, the daily repeatability also suggests carrier phase multipath effects, since the QZSS satellite has basically identical observation geometry for each pass. The triple-frequency pseudorange and carrier phase combinations do not exhibit obvious systematic variations, which are correlated among the receivers. It can therefore be concluded that satellite-dependent line biases have a sufficient stability to not exceed errors like multipath and receiver noise.

### Yaw attitude profile

The SAIF signal has not been considered in the previous analysis, since it is intended as a signal with correction data rather than a ranging signal. Its dedicated antenna is mounted with an offset of about 1.34 m with respect to the main antenna. This feature can be exploited to estimate the yaw attitude of Michibiki. The method is essentially an inversion of the GNSS-based attitude determination problem, where the orientation of a baseline between two antennas on the ground is estimated using differential

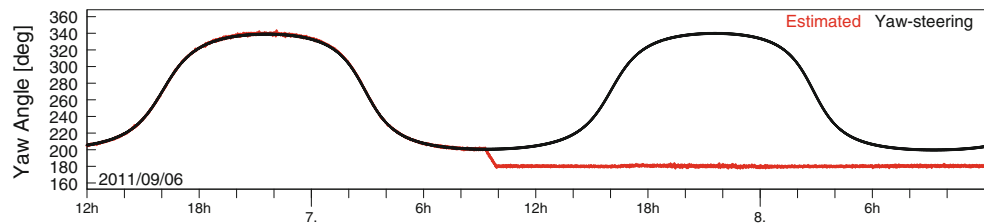
measurements from different satellites. In this case, the baseline between the L-band main antenna and the SAIF antenna is estimated based on differences between SAIF and C/A (or L1C) carrier phase observation from different stations (Hauschild et al. 2011).

Contrary to GPS and GLONASS, QZSS uses two different attitude modes depending on the sun's elevation angle  $\beta$  with respect to the orbital plane. For  $|\beta| > 20^\circ$ , the standard yaw-steering attitude profile is used. In this mode, the satellite's body-fixed z-axis points toward the center of the earth, and the satellite is rotated such that the solar panels are oriented normally to the sun vector (Bar-Sever 1996). However, for  $|\beta| < 20^\circ$ , the satellite switches to orbit-normal orientation, in which the solar panel axis is oriented normally to the orbital plane and the body-fixed z-axis points toward the earth (Inaba et al. 2009). Using a different attitude mode for small  $\beta$  eliminates the need to rotate the spacecraft with high yaw rates, which can exceed the maximal possible hardware yaw rate if  $\beta$  is close to zero. However, the different attitude modes must be taken into account when processing carrier phase observations of QZSS for high-precision applications. Otherwise, the phase wind-up effect can lead to inconsistencies between the observed and modeled carrier phases if an improper attitude model is used. Moreover, the SLR reflector array is not aligned with the center of mass of the satellite, such that attitude errors would appear in the residuals of SLR measurements.

Figure 6 depicts the yaw angle corresponding to yaw-steering mode in black together with estimated values in red over a time period of 48 h. During this period, a switch from yaw steering to orbit-normal attitude takes place at about 09:20 h GPST on September 7, 2011. It is interesting



**Fig. 6** Estimated (red) and modeled (black) yaw attitude of QZS-1 for a 48-h period centered at Sept. 7, 2011. The attitude mode switch from yaw-steering to orbit-normal orientation starts at 09:20 h UTC on Sept. 7



to note that the switch already starts when  $\beta$  is at approximately  $20.59^\circ$ . The threshold of  $20^\circ$  is not reached until 01:20 h GPST on the following day.

The reason for performing the maneuver prior to exceeding the threshold is immediately obvious, since the satellite is closest to its final orientation at this point in time. Similar results have also been found for yaw attitude estimations during the entry and exit of the previous shadow period in spring 2011. However, the exit maneuver in April 2011 has already been executed 34 h prior to exceeding the threshold. With the help of yaw angle estimates, profiles of the actual satellite attitude can be derived to remove the uncertainty at which point in time the switch has exactly been performed.

### Orbit determination

The GPS and QZSS observations of the five CONGO stations are used for an orbit determination on a daily basis. The processing scheme is similar to that of GIOVE-B discussed in Steigenberger et al. (2011). A modified version of the Bernese GPS Software (Dach et al. 2007) is used to process dual-frequency GPS and QZSS tracking data. In a first step, station positions, troposphere parameters and epoch wise receiver clock offsets are estimated with GPS data only using the CODE (Center for Orbit Determination in Europe) rapid orbit and satellite clock products. The IF linear combination of L1 and L2 is used for GPS, while that of L1 and L5 is used for QZSS. Code and phase observations are processed simultaneously. The parameters estimated in the first step are kept fixed in the second step, the QZS-1 orbit and clock determination. Epoch wise QZS-1 satellite clock offsets, six Kepler elements and five radiation pressure parameters of the Beutler et al. (1994) model are estimated per day. In addition to the 1-day solution computed with a latency of about 16 h, a 5-day solution is computed to achieve a higher stability of the satellite orbits by stacking the orbital elements and radiation parameters of the five consecutive days. In the 5-day solution, the full set of nine radiation pressure parameters according to Beutler et al. (1994) is estimated.

A time period of 2 weeks (DOY 217–230 of 2011) has been considered for the following analysis. The median of daily RMS values for phase and code residuals of the orbit

and clock determination are given in Table 1. Since the noise of observations increases with decreasing elevation, the magnitude of the residuals largely depends on the visibility conditions of QZS-1 at the corresponding stations shown in Fig. 7. For MAHO and THTX, there are no observations above  $30^\circ$ , whereas almost all observations of SING have a larger elevation than  $30^\circ$  resulting in the smallest phase residuals. Contrary to the other stations, which provide continuous tracking, MAHO and THTX have QZS-1 visibility periods limited to about 17 and 10 h, respectively. As these periods are dominated by observations with low elevations, the residuals are larger by a factor of up to five compared with the other stations. The reason for the increased phase residuals at CHOF is unknown.

Since observations of different navigation systems (GPS and QZSS) and different frequencies (L1/L2 and L1/L5) are processed together, the biases between the code observations have to be considered. This is done by estimating differential code biases (DCBs) for all stations except for CHOF, which is constrained to zero. The mean biases (composed of inter-system and inter-frequency biases) are listed in Table 1. The biases are in the order of a few nanoseconds corresponding to less than one meter expressed in range with a standard deviation usually better than half a nanosecond. Compared with the GIOVE (Galileo In Orbit Validation Element) biases also estimated from the CONGO network, the QZSS biases are up to one order of magnitude smaller.

The differences between the orbits estimated from the CONGO network and the broadcast orbits provided by JAXA are shown in Fig. 8. The mean differences are  $-0.58$ ,  $-0.36$  and  $1.41$  m in radial, cross-track and along-track

**Table 1** Station-specific residuals and code biases from the orbit and clock determination

Station	Residuals (median)		DCB (ns)
	Phase (cm)	Code (cm)	
CHOF	3.7	35.3	Fixed to zero
MAHO	1.7	56.5	$-0.96 \pm 0.49$
SING	1.1	40.4	$0.61 \pm 0.24$
THTX	5.5	154.3	$2.47 \pm 0.54$
UNSX	1.7	63.1	$0.28 \pm 0.21$

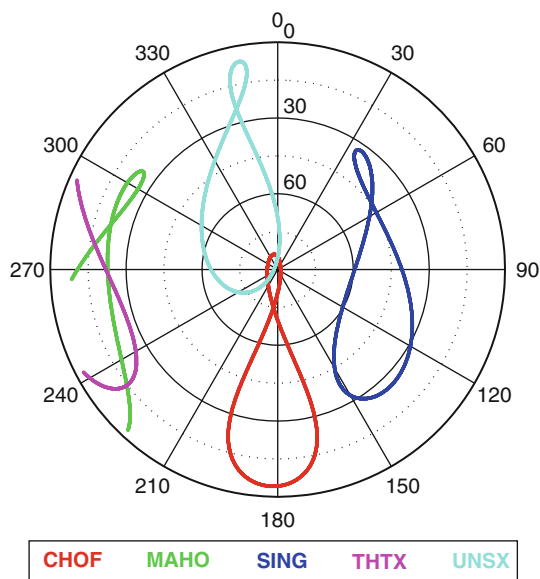


**Fig. 7** QZS-1 visibility of the five CONGO stations in corresponding local horizontal systems

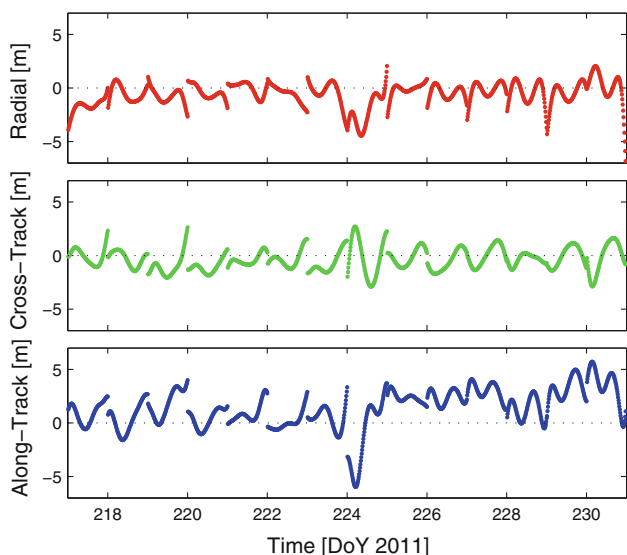


**Fig. 8** Differences between QZS-1 1-day orbits estimated from the CONGO network and broadcast orbits

direction with standard deviations of 1.10, 1.04 and 1.82 m, respectively. As the CONGO orbits are computed from 1 day of data, the largest differences occur at the day boundaries. Two different measures for the internal consistency of the orbits are given in Table 2. The 2-day orbit fit RMS is the RMS of two consecutive orbital arcs with respect to a 2-day orbit fitted through the original orbits with the orbital model mentioned above. Since the CONGO orbits were computed with the same orbital model, it is not surprising that the RMS is smaller compared with the broadcast orbits. The very small RMS of 3.5 cm for the

**Table 2** Orbit fit residuals and day boundary discontinuities for different orbit types

	Broadcast	CONGO 1-day	CONGO 5-day
2-day orbit fit RMS	126	55	3.5
Day boundary discontinuities	75	449	16

Units are in centimeters

5-day orbits can be explained by the usage of overlapping data intervals for the computation of the 5-day orbits. The day boundary discontinuities given in Table 2 are the 3D position differences between two orbits at the midnight epoch. The CONGO 1-day orbits are completely independent from each other resulting in the largest day boundary discontinuities of almost 4.5 m. The discontinuities of the broadcast orbits are smaller by a factor of six compared with the 1-day orbits. This is due to the fact that broadcast ephemerides are fitted to orbit predictions with sufficient overlap to ensure smooth transitions. The longer data interval used for the CONGO 5-day orbits resulting in a smoothing is responsible for the smallest day boundary discontinuities of 16 cm for this orbit type. Based on the orbit comparisons and numerical values given in Table 2, the orbit accuracy is assumed to be at the few meter level. A meaningful analysis of satellite laser ranging measurements could not be performed since only 17 normal points from a single tracking station are available for the test interval.

**Conclusions**

Results were presented for Japan’s first navigation satellite Michibiki, which is the first satellite of a new regional navigation system. Five stations of the CONGO network have been upgraded with QZSS-capable firmware and provide measurements for five of the six signals transmitted by the spacecraft. The carrier-to-noise density ratios of QZSS and GPS have been compared for a receiver in Chofu, Japan. It is interesting to note that contrary to GPS, the path loss of QZSS varies by about 1.5 dB due to the eccentricity of the orbit. The code multipath has been assessed from the multipath combination for two stations. A similar multipath performance is expected for GPS and QZSS, since both systems use the same signal structure. This result can be confirmed for L1 and L2 signals. For L5, however, the single GPS satellite contributing to the statistics is affected by larger multipath errors compared with QZSS at both stations. The triple-frequency combination of the pseudorange and carrier phase observations is stable over a period of 1 week, which suggests that no notable line bias variations are present onboard the spacecraft.

One of the unique features of QZSS compared with other navigation satellite systems is the transmission of an L1 signal (SAIF) from a dedicated antenna mounted with an offset to the main L-band antenna, which allows the estimation of the satellites yaw attitude. Estimation results for an attitude mode switch from yaw-steering to orbit-normal orientation are presented.

The orbit determination accuracy for QZS-1 based on the small network of only five stations has been assessed to be on the order of a few meters. Differential code biases have been estimated in order to process GPS L1/L2 signals and QZSS L1/L5 signals together consistently. The biases are on the order of a few nanoseconds.

## References

- Bar-Sever YE (1996) A new model for GPS yaw attitude. *J Geodesy* 70(11):714–723. doi:[10.1007/BF00867149](https://doi.org/10.1007/BF00867149)
- Beutler G, Brockmann E, Gurtner W, Hugentobler U, Mervart L, Rothacher M, Verdun A (1994) Extended orbit modeling techniques at the CODE processing center of the international GPS service for Geodynamics (IGS): theory and initial results. *Manuscripta Geodaetica* 19:367–386
- Dach R, Hugentobler U, Fridez P, Meindl M (eds) (2007) *Bernese GPS software version 5.0*. Astronomical Institute, University of Bern, Bern
- Hauschild A, Steigenberger P, Rodriguez-Solano C (2011) QZS-1 yaw attitude estimation based on measurements from the CONGO network. *ION GNSS Conference*, 20–23 Sep 2011, Portland
- Inaba N, Matsumoto A, Hase H, Kogure S, Sawabe M, Terada K (2009) Design concept of quasi zenith satellite system. *Acta Astronautica* 65(7–8):1068–1075. doi:[10.1016/j.actaastro.2009.03.068](https://doi.org/10.1016/j.actaastro.2009.03.068)
- Kee C, Parkinson B (1994) Calibration of multipath errors on GPS pseudorange measurements. In: *Proceedings of the 7th international technical meeting of the satellite division of the institute of navigation*, Salt Lake City, 20–23 Sep 1994, pp 353–362
- Kishimoto M, Noda H, Kogure S, Sawabe M, Terada K (2011) QZSS on orbit technical verification results. *ION GNSS Conference*, 20–23 Sep 2011, Portland
- Montenbruck O, Hauschild A, Hessels U (2011a) Characterization of GPS/GIOVE sensor stations in the CONGO network. *GPS Solut* 15(3):193–205. doi:[10.1007/s10291-010-0182-8](https://doi.org/10.1007/s10291-010-0182-8)
- Montenbruck O, Hugentobler U, Dach R., Steigenberger P, Hauschild A (2011b) Apparent clock variations of the block IIF-1 (SVN62) GPS satellite. *GPS Solut*. doi: [10.1007/s10291-011-0232-x](https://doi.org/10.1007/s10291-011-0232-x)
- Saito M, Sato Y, Miya M, Omura Y, Shima M, Yoshino T, Asari K (2011) Centimeter-class augmentation system utilizing quasi-zenith satellite. *ION GNSS Conference*, 20–23 Sep 2011, Portland
- Steigenberger P, Hugentobler U, Montenbruck O, Hauschild A (2011) Precise orbit determination of GIOVE-B based on the CONGO Network. *J Geodesy* 85(6):357–365. doi:[10.1007/s00190-011-0443-5](https://doi.org/10.1007/s00190-011-0443-5)

## Author Biographies



**André Hauschild** is a scientific staff member at DLR's German Space Operations Center (GSOC). His field of work focuses on precise real-time orbit and clock estimation for GNSS satellites as well as multi-GNSS processing using modernized GPS and new satellite navigation systems.



**Peter Steigenberger** works at the Institute of Astronomical and Physical Geodesy of Technische Universität München (TUM, Munich, Germany). His current research interests include global GNSS solutions and the analysis of the GNSS-derived parameter time series, e.g., troposphere zenith delays, station coordinates, satellite orbits and Earth rotation parameters.



**Carlos Rodriguez-Solano** is a Ph.D. student at the Institute of Astronomical and Physical Geodesy of Technische Universität München, currently working on the impact of non-conservative force modeling on GNSS satellite orbits.